2021 10th International IEEE/EMBS Conference on Neural Engineering (NER)
Virtual Conference, May 4-6, 2021

Model neocortical microcircuit supports beta and gamma rhythms

Feng Feng, Drew B. Headley, and Satish S. Nair, *Member, IEEE*

Abstract— **Gamma and beta rhythms in neocortical circuits are thought to be caused by distinct subcircuits involving different type of interneurons. However, it is not clear how these distinct but inter-linked intrinsic circuits interact with afferent drive to engender the two rhythms. We report a biophysical computational model to investigate the hypothesis that tonic and phasic drive might engender beta and gamma oscillations, respectively, in a neocortical circuit.**

I. Introduction

Brain rhythms are typically measured using non-invasive scalp and subdural electrodes for humans and implanted multi-electrode arrays for rodents and non-human primates. These electrodes pick up extracellular potentials that reflect cellular electrical activities. Depending on the recording locations, extracellular potentials can be referred into encephalogram (EEG, recorded from the scalp), electrocorticogram (ECoG, recorded on cortical surface), and local field potential (LFP, recorded inside the brain). Among these, LFP has the advantage of exploring localized cellular events at deeper locations, since it is obtained when electrode placed closer to the generating cells. One such event is the rhythmicity in neuronal activity that can typically be detected in LFP signals.

Computational models of brain rhythms are beginning to provide important insights into the underlying microcircuits that might implement these rhythms in neuronal circuits. For instance, the gamma (30-90Hz) rhythm is thought to arise *in vivo* via feedback interactions between pyramidal cells (PNs) and fast spiking inhibitory (FSI) interneurons (termed pyramidal-interneuron-gamma or PING). The models also suggest conditions for the genesis of the rhythms, e.g., for the PING mechanism, excitatory drive to the interneurons has to largely come from pyramidal cells [1]. On the other hand, beta (15-30Hz) oscillation is thought to arise from either an interaction between pyramidal cells[2] or an interaction between pyramidal and low threshold-spiking (LTS) cells [3]. The long-lasting IPSPs from oriens-lacunosum moleculare (OLM) cells was found to be the critical element supporting another slower oscillation rhythm – theta (4-12Hz) [4].

Computational models thus enable exploration of how the microcircuits underlying different rhythms can give rise to different abilities of a network to form and manipulate cell assemblies [5]. Furthermore, such models can shed light on how the circuits might implement computations, enable information flow across brain regions, and possibly support components of cognition [6].

Recent experimental work has underscored the importance of FSI and LTS neurons in the generation of gamma and beta oscillations, respectively [3]. At the same time, models have emphasized the role of these interneurons in synchronizing activities or selecting ensembles [6]. However, it remains unclear how interneuron networks and their resultant rhythms interact with the patterns of ensemble activity, and how they influence excitatory networks subjected to naturalistic afferent drive.

Rhythms are a critical determining factor in the formation of cell ensemble patterns, and different rhythms are associated with different underlying physiology [6]. The present study uses a computational network model to test whether different patterns of afferent drive representing distinct behavioral states, can engender and shape different ensemble oscillations.

The specific computational example case considered here was motived by recordings from the primary motor cortex M1 that reveals both beta and gamma oscillations during the preparation and execution phases of movement. Beta oscillations dominate during the preparatory phase. It was traditionally thought that these were inherited from the basal ganglia [7], however slices of motor cortex in vitro are capable of generating beta when supplied with tonic excitation pharmacologically [8]. Indeed, biophysical models of M1 circuitry given tonic excitation produce beta oscillations that are consistent with those from human magnetoencephalographic recordings [9]. M1 beta rhythms may co-occur with periods of tonic activity because they are mediated by LTS interneurons [3], which are sensitive to slow changes in local firing rates. This arises because they receive weak, but facilitating, synapses from local principal cells. Facilitating synapses require trains of presynaptic activity – the kind present during tonic firing – to effectively drive spiking. Once excited, LTS interneurons target PN dendritic branches, causing a gradual inhibition [10].

Once movement begins ensemble activity rapidly fluctuates, accompanied by gamma oscillations [11]. Gamma oscillations arise locally from the reciprocal interactions between PNs and FSIs [3], and both *in vitro* and *in vivo* experiments have validated this perspective in M1[12]. Since FSIs receive strong, but depressing excitatory synapses from principal cells, have a fast membrane time constant, and deliver robust periosomatic inhibition capable of rapidly cancelling principal cell spiking, they are sensitive to rapid shifts in the pattern of presynaptic activity [13].

F Feng and SS Nair are with the Department of Electrical Engineering and Computer Science, University of Missouri, Columbia MO 65211 (corresponding author SSN phone: 573-882-2964; fax: 573-882-0397; e-mail: nairs@missouri.edu).

DH Headley is a Research Associate with the Center for Molecular and Behavioral Neuroscience, Rutgers University, Newark, NJ 07102.

This research was supported in part by This research was supported in part by grants NIH MH122023 and NSF OAC-1730655 to SSN.

2021 10th International IEEE/EMBS Conference on Neural Engineering (NER) | 978-1-7281-4337-8/21/$31.00 ©2021 IEEE | DOI: 10.1109/NER49283.2021.9441199

Although different populations of interneurons support beta and gamma, they share the same local principal cell network. Principal cells densely project to FSI and LTS interneurons, which in turn promiscuously and indiscriminately reciprocate those connections [14]. Consequently, both interneuron types receive a similar aggregate excitatory signal, and they broadcast their feedback inhibition to all nearby principal cells [15]. This lack of specificity indicates that inhibitory connectivity regulates overall excitability in M1 during different activity modes, but the distinct ensemble patterns therein arise from the excitatory connections amongst principal cells and their extrinsic inputs.

II. Method

Models of single neurons and the network were developed using experimental parameters from our collaborators and the literature, and implemented using the NEURON 7.4 simulator [16], with a fixed time step of 25 µs. We provide a brief overview of the mathematical underpinnings of both single cell and network model development.

Mathematical equations for voltage-dependent ionic currents: The dynamics for each compartment (soma or dendrite) followed the Hodgkin-Huxley formulation as previously described [17] in eqn. 1,

$$C_m dV_s/dt = -g_L(V_s - E_L) - g_c(V_s - V_d) - \sum I_{cur,s}^{int} - \sum I_{cur,s}^{syn} + I_{inj} \quad (1)$$

where V_s/V_d are the somatic/dendritic membrane potential (mV), $I_{cur,s}^{int}$ and $I_{cur,s}^{syn}$ are the intrinsic and synaptic currents in the soma, I_{inj} is the electrode current applied to the soma, C_m is the membrane capacitance, g_L is the conductance of the leak channel, and g_c is the coupling conductance between the soma and the dendrite (similar term added for other dendrites connected to the soma). The intrinsic current $I_{cur,s}^{int}$, was modeled as $I_{cur,s}^{int} = g_{cur} m^p h^q (V_s - E_{cur})$, where g_{cur} is its maximal conductance, m its activation variable (with exponent p), h its inactivation variable (with exponent q), and E_{cur} its reversal potential (a similar equation is used for the synaptic current $I_{cur,s}^{syn}$ but without m and h). The kinetic equation for each of the gating variables x (m or h) takes the form but without m and h). The kinetic equation for each of the gating variables x (m or h) takes the form

$$\frac{dx}{dt} = \frac{x_\infty\left(V,[Ca^{2+}]_i\right) - x}{\tau_x(V,[Ca^{2+}]_i)} \quad (2)$$

where x_∞ is the steady state gating voltage- and/or Ca^{2+}-dependent gating variable and τ_x is the voltage- and/or Ca^{2+}-dependent time constant. The equation for the dendrite follows the same format with 's' and 'd' switching positions in eqn. 1. Selection of the channel currents and their model parameters followed an approach we proposed recently that facilitates design while ensuring that the key neurocomputational properties of the cell are preserved [18].

Single cell models. The single cells were of two overall classes, principal cells (PNs), and GABAergic interneurons [17]. The PNs have three compartments and are based on corticopontine neurons. These three compartments representing a soma (diameter, 24.75 µm; length, 25 µm), an apical dendrite (a-dend; diameter, 3 µm and length, 270 µm) and another basal dendrite (p-dend; diameter, 5 µm and length, 555 µm). These cells receive short term depressing synapses from local FS interneurons. Model parameters for PN were tuned to match passive properties and current-clamp spiking behaviors from experimental results found in [19, 20]. FSI model is comprised of a soma compartment (diameter, 15 µm; length, 15 µm) and a dendrite compartment (diameter, 15 µm; length, 150 µm). LTS model has three compartments: a soma (diameter, 20 µm; length, 10 µm), an apical dendrite (a-dend; diameter, 3 µm and length, 250 µm) and another basal dendrite (p-dend; diameter, 3 µm and length, 250 µm) (Fig 1A). Model parameters for both FS and FSI were tuned to match passive properties and current-clamp spiking behaviors from experimental results found in [20] (Fig 2A). Our model uses multi-compartment single cell models for two reasons. First, we calculate LFP using first principles [17] necessitating such models [21]. Second, LTS neurons synapse onto apical dendrites of pyramidal cells [22].

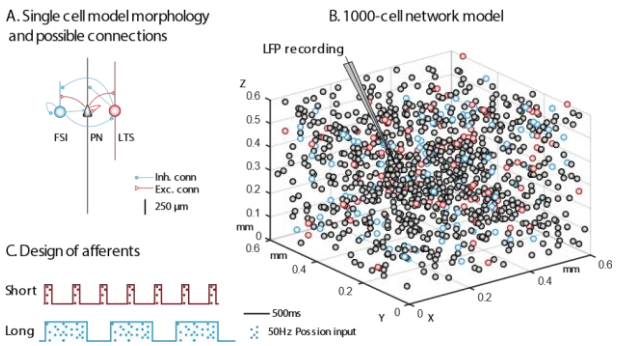

Figure 1 A. Modeling morphology for three single cells with 8 possible synaptic connections. **B.** The placement of 1000 cells in space (with only soma locations displayed). **C.** Schematic for the afferents to the network.

Network connectivity. We developed a 1000-cell network model comprising 800 PNs, 100 FSs and 100 FSIs (Fig 1B). Except for FSI→ FSI connections with both electrical and chemical synapses, all other connections had chemical synapses (Fig 1A, dash lines). Connection probability were based on the following reports: [20, 23, 24].

Synaptic currents. Excitatory transmission was mediated by AMPA/NMDA receptors, and inhibitory transmission by $GABA_A$ receptors. Model AMPA and GABA synapses also exhibited short term pre-synaptic plasticity (STP) between FSI and PN and from PN to FSI, as in our previous models [25] (Fig. 2B): For facilitation, the factor F was calculated using the equation: $\tau_F * dF/dt = 1 - F$ and was constrained to be ≤ 10. After each stimulus, F was multiplied by a constant, f (≥1) representing the amount of facilitation per pre-synaptic action potential (AP), and updated as $F \rightarrow F*f$. Between stimuli, F recovered exponentially back toward 1. A similar scheme was used to calculate the factor D for depression: $\tau_D * dD/dt = 1 - D$. After each stimulus, D was multiplied by a constant d (≤ 1) representing the amount of depression per pre-synaptic AP, and updated as $D \rightarrow D*d$. Between stimuli,

Table 1. Parameters related to STP

Connection	STP type	Parameters		
		D or F (Max. limit)	d_1/d_2 or f	τ_{D1} / τ_{D2} or τ_F (ms)
FSI→PN	depressing	1	0.7 / 1	300 / 1
PN→FSI	depressing	1	0.6 / 0.5	300 / 20
PN→LTS	facilitating	10	1.5	150

D recovered exponentially back towards 1. We modeled depression using two factors d_1 and d_2 with d_1 being fast and d_2 being slow subtypes, and $d = d_1 * d_2$. The parameters for the STP are listed in Table 1.

Inputs. Afferent activity was simulated by delivering excitatory synaptic drive as a Poisson process at 50 Hz to 12.5% of PNs (representing ensembles). Trains of afferent activity were delivered for 200 ms followed by 500ms of silence, to simulate transient drive. For tonic drive, activation persisted for 1000 ms followed by 500 ms of silence (Fig 1C).

Calculation of LFP. We recorded transmembrane ionic currents from each compartment of the model cells using the extracellular mechanism in NEURON [16]. The extracellular potential arising from each neuronal compartment was then calculated using the line source approximation method, which provides a better approximation than point sources [21].

III. Results

To establish the validity of our model neurons, we delivered 300 pA current steps to them and examined their spiking patterns (Fig. 2A). The CP neuron, which is of the regular spiking type, exhibited a low firing frequency during the current pulse without adaptation. On the other hand, both the FSI and LTS interneurons exhibited higher induced firing rates, with the FSI cell exhibiting the fast-spiking phenotype that typifies them. However, the LTS neuron only fired continuously for the highest current level with slight adaptation. We also examined the short-term synaptic plasticity of the connections between these cell types (Fig. 2B). The FSI-to-CP GABAergic synapses showed depression, a weakening of inhibition during repeated spiking. The same was true for the glutamatergic synapse from CP-to-FSI. On the other hand, synapses from CP-to-LTS were facilitating, increasing in strength during trains of spikes.

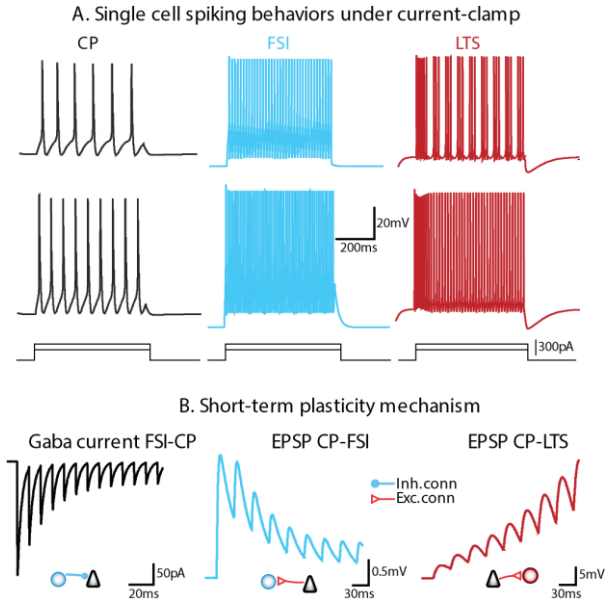

Figure 2 A. Spiking pattern from single cell model under current clamp. **B.** Short-term plasticity mechanism was incorporated into FSI->CP, CP-> FSI and CP->LTS.

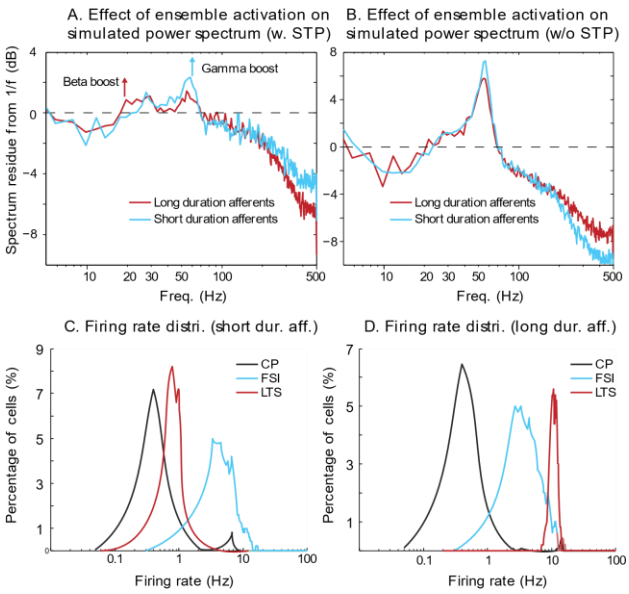

Figure 3 A. Power spectrum comparison when model was driven with different afferents. **B.** Same comparison as A, but STP was removed. **C.** Firing rate distribution when model was driven with short duration afferents. **D.** Same as C, but when model was driven with long duration afferents.

Having established that our single cell and synapse models match the biological case, we turned our attention to their network effects. Driving the network with short bursts of afferent activity drove relatively stronger gamma centered around 60Hz. Driving with long duration bursts reduced gamma power, but enhanced beta around 20Hz. (Fig. 3A). The average firing rate for each cell type is (Fig. 3C and D): CP,1.37±2.02Hz (hereafter, mean ± std), FSI, 5.75±2.93Hz and LTS, 0.86±0.30Hz, when network was driven with short duration afferents; CP,2.31±4.42Hz, FSI, 5.33±2.97Hz and LTS, 10.78±1.33Hz, when network was driven with long duration afferents. Average firing rate is within the experimental range [26]. Importantly, this phenomenon was not observed when the STP mechanism was removed from the model, suggesting the critical role of STP underlying the collaboration between two oscillations. This further indicates that, beta oscillation is related closely to stable activities like preparation, while gamma is more linked to dynamic activities like movement onset.

IV. Discussion and Conclusion

We have tested the importance of STP in the generation of neural oscillations. Our hypothesis was that because FSI neurons receive depressing synapses, and they are instrumental in producing gamma oscillations, then rapidly fluctuating ensembles would be ideal for gamma genesis. In addition, because LTS neurons receive facilitating synapses from CP neurons, and engender beta oscillations, then tonically active ensembles would induce beta. These dependencies were borne out in our model.

Previous work on gamma and beta oscillations have emphasized the resonant properties of interneuron networks [3, 9] as being instrumental in rhythm generation. Our work indicates that this is only part of the reason for the emergence of brain rhythms. The frequency of the rhythm is largely determined by the resonance of the recurrent principal cells/interneuron network. However, whether that network is activated, and the persistence of that activity, depends upon the slower temporal dynamics of the principal cell ensembles that supply the excitation to fuel the rhythm. This insight opens up new avenues for experimental and theoretical investigations into the function of rhythms in the brain.

References

[1] C. Borgers and N. Kopell, "Effects of noisy drive on rhythms in networks of excitatory and inhibitory neurons," *Neural Comput,* vol. 17, no. 3, pp. 557-608, Mar 2005, doi: 10.1162/0899766053019908.

[2] N. Kopell, G. B. Ermentrout, M. A. Whittington, and R. D. Traub, "Gamma rhythms and beta rhythms have different synchronization properties," *Proceedings of the National Academy of Sciences of the United States of America,* vol. 97, no. 4, pp. 1867-72, Feb 15 2000, doi: 10.1073/pnas.97.4.1867.

[3] G. Chen *et al.*, "Distinct Inhibitory Circuits Orchestrate Cortical beta and gamma Band Oscillations," *Neuron,* vol. 96, no. 6, pp. 1403-1418 e6, Dec 20 2017, doi: 10.1016/j.neuron.2017.11.033.

[4] M. J. Gillies *et al.*, "A model of atropine-resistant theta oscillations in rat hippocampal area CA1," *J Physiol,* vol. 543, no. Pt 3, pp. 779-93, Sep 15 2002, doi: 10.1113/jphysiol.2002.024588.

[5] K. D. Harris, J. Csicsvari, H. Hirase, G. Dragoi, and G. Buzsaki, "Organization of cell assemblies in the hippocampus," *Nature,* vol. 424, no. 6948, pp. 552-6, Jul 31 2003, doi: 10.1038/nature01834.

[6] N. Kopell, M. A. Kramer, P. Malerba, and M. A. Whittington, "Are different rhythms good for different functions?," *Front Hum Neurosci,* vol. 4, p. 187, 2010, doi: 10.3389/fnhum.2010.00187.

[7] A. J. Holgado, J. R. Terry, and R. Bogacz, "Conditions for the generation of beta oscillations in the subthalamic nucleus-globus pallidus network," *The Journal of neuroscience : the official journal of the Society for Neuroscience,* vol. 30, no. 37, pp. 12340-52, Sep 15 2010, doi: 10.1523/JNEUROSCI.0817-10.2010.

[8] M. G. Lacey *et al.*, "Spike firing and IPSPs in layer V pyramidal neurons during beta oscillations in rat primary motor cortex (M1) in vitro," *PLoS One,* vol. 9, no. 1, p. e85109, 2014, doi: 10.1371/journal.pone.0085109.

[9] M. A. Sherman *et al.*, "Neural mechanisms of transient neocortical beta rhythms: Converging evidence from humans, computational modeling, monkeys, and mice," *Proceedings of the National Academy of Sciences of the United States of America,* vol. 113, no. 33, pp. E4885-94, Aug 16 2016, doi: 10.1073/pnas.1604135113.

[10] C. Kapfer, L. L. Glickfeld, B. V. Atallah, and M. Scanziani, "Supralinear increase of recurrent inhibition during sparse activity in the somatosensory cortex," *Nature neuroscience,* vol. 10, no. 6, pp. 743-53, Jun 2007, doi: 10.1038/nn1909.

[11] M. M. Churchland *et al.*, "Neural population dynamics during reaching," *Nature,* vol. 487, no. 7405, pp. 51-6, Jul 5 2012, doi: 10.1038/nature11129.

[12] N. W. Johnson *et al.*, "Phase-amplitude coupled persistent theta and gamma oscillations in rat primary motor cortex in vitro," *Neuropharmacology,* vol. 119, pp. 141-156, Jun 2017, doi: 10.1016/j.neuropharm.2017.04.009.

[13] Y. Kawaguchi, T. Otsuka, M. Morishima, M. Ushimaru, and Y. Kubota, "Control of Excitatory Hierarchical Circuits by Parvalbumin-FS Basket Cells in Layer 5 of the Frontal Cortex: Insights for Cortical Oscillations," *Journal of neurophysiology,* Apr 17 2019, doi: 10.1152/jn.00778.2018.

[14] A. M. Packer and R. Yuste, "Dense, unspecific connectivity of neocortical parvalbumin-positive interneurons: a canonical microcircuit for inhibition?," *The Journal of neuroscience : the official journal of the Society for Neuroscience,* vol. 31, no. 37, pp. 13260-71, Sep 14 2011, doi: 10.1523/JNEUROSCI.3131-11.2011.

[15] E. Fino, A. M. Packer, and R. Yuste, "The logic of inhibitory connectivity in the neocortex," *The Neuroscientist : a review journal bringing neurobiology, neurology and psychiatry,* vol. 19, no. 3, pp. 228-37, Jun 2013, doi: 10.1177/1073858412456743.

[16] N. T. Carnevale and M. L. Hines, *The NEURON book*. Cambridge ; New York: Cambridge University Press, 2005, pp. xix, 457 p.

[17] F. Feng *et al.*, "Gamma oscillations in the basolateral amygdala: biophysical mechanisms and computational consequences," pp. ENEURO.0388-18.2018, 2019, doi: 10.1523/ENEURO.0388-18.2018 %J eneuro.

[18] A. Alturki, F. Feng, A. Nair, V. Guntu, and S. S. Nair, "Distinct current modules shape cellular dynamics in model neurons," *Neuroscience,* vol. 334, pp. 309-331, Oct 15 2016, doi: 10.1016/j.neuroscience.2016.08.016.

[19] G. T. Neske, S. L. Patrick, and B. W. Connors, "Contributions of diverse excitatory and inhibitory neurons to recurrent network activity in cerebral cortex," *The Journal of neuroscience : the official journal of the Society for Neuroscience,* vol. 35, no. 3, pp. 1089-105, Jan 21 2015, doi: 10.1523/JNEUROSCI.2279-14.2015.

[20] M. Beierlein, J. R. Gibson, and B. W. Connors, "Two dynamically distinct inhibitory networks in layer 4 of the neocortex," (in English), *Journal of neurophysiology,* vol. 90, no. 5, pp. 2987-3000, Nov 1 2003, doi: 10.1152/jn.00283.2003.

[21] G. T. Einevoll, C. Kayser, N. K. Logothetis, and S. Panzeri, "Modelling and analysis of local field potentials for studying the function of cortical circuits," *Nature reviews. Neuroscience,* vol. 14, no. 11, pp. 770-85, Nov 2013, doi: 10.1038/nrn3599.

[22] S. B. Wolff *et al.*, "Amygdala interneuron subtypes control fear learning through disinhibition," *Nature,* vol. 509, no. 7501, pp. 453-8, May 22 2014, doi: 10.1038/nature13258.

[23] T. Kiritani, I. R. Wickersham, H. S. Seung, and G. M. Shepherd, "Hierarchical connectivity and connection-specific dynamics in the corticospinal-corticostriatal microcircuit in mouse motor cortex," *The Journal of neuroscience : the official journal of the Society for Neuroscience,* vol. 32, no. 14, pp. 4992-5001, Apr 4 2012, doi: 10.1523/JNEUROSCI.4759-11.2012.

[24] M. Morishima, K. Kobayashi, S. Kato, K. Kobayashi, and Y. Kawaguchi, "Segregated Excitatory-Inhibitory Recurrent Subnetworks in Layer 5 of the Rat Frontal Cortex," *Cerebral cortex,* vol. 27, no. 12, pp. 5846-5857, Dec 1 2017, doi: 10.1093/cercor/bhx276.

[25] A. Hummos, C. C. Franklin, and S. S. Nair, "Intrinsic mechanisms stabilize encoding and retrieval circuits differentially in a hippocampal network model," *Hippocampus,* vol. 24, no. 12, pp. 1430-48, Dec 2014, doi: 10.1002/hipo.22324.

[26] J. Urban-Ciecko and A. L. Barth, "Somatostatin-expressing neurons in cortical networks," *Nature reviews. Neuroscience,* vol. 17, no. 7, pp. 401-9, Jul 2016, doi: 10.1038/nrn.2016.53.